NIH Public Access
Author Manuscript
Electroanalysis. Author manuscript; available in PMC 2012 October 01.

Published in final edited form as:
Electroanalysis. 2011 October ; 23(10): 2357–2363. doi:10.1002/elan.201100348.

Nanomolar Detection of Glutamate at a Biosensor Based on Screen-Printed Electrodes Modified with Carbon Nanotubes

Raju Khan[a,b], **Waldemar Gorski**[b], and **Carlos D. Garcia**[b,*]

[a]Analytical Chemistry Division, North East Institute of Science & Technology, Jorhat, 785006, Assam, India

[b]Department of Chemistry, The University of Texas at San Antonio, One UTSA Circle, San Antonio, TX, 78249, United States of America

Abstract

The amperometric glutamate biosensor based on screen-printed electrodes containing carbon nanotubes (CNT), and its integration in a flow injection analysis system, is described herein. The sensor was fabricated by simply adsorbing enzyme glutamate oxidase (GlutOx) on a commercial substrate containing multi-wall CNT. The resulting device displayed excellent electroanalytical properties toward the determination of L-glutamate in a wide linear range (0.01–10 μM) with low detection limit (10 nM, S/N≥3), fast response time (≤5 s), and good operational and long-term stability. The CNT modified screen-printed electrodes have a potential to be of general interest for designing of electrochemical sensors and biosensors.

Keywords

Amperometry; L-Glutamate; Glutamate oxidase; Flow Injection Analysis; Carbon Nanotubes

1. INTRODUCTION

Biosensors have been applied in many fields including clinical diagnostics, food processing and biomedical research. Typically, biosensors provide a selective way of assessing the concentration of a given molecule of interest. Among others, the analysis of L-glutamate has received much attention recently. L-glutamate (Glut) is one of the most commonly found amino acids in nature [1] and has critical neurological functions, particularly as a neurotransmitter.[2, 3] Glutamate is also an important flavor enhancer (MSG, monosodium glutamate), typically added to processed meats, poultry, seafood, snacks, soups and stews at a concentration ranging from 0.1 to 0.8 wt.%. [4] Although most regulatory agencies have affirmed the safety of L-glutamate at levels normally consumed by the general population, most customers have the perception that glutamate may have detrimental health effects. [4] In response to such perception and due to the important biological functions of L-glutamate, various instrumental methods have been developed for its analysis, liquid chromatography being amongst the most popular ones. [5, 6] However, this technique is typically time consuming, generates large volumes of waste, and requires relatively skilled personnel. Hence, developing alternative means for such analysis is understandably appealing to the analytical community.

Several alternative approaches have been developed to quantify L-glutamate including methods based on capillary electrophoresis, [7] chemiluminometry, [8] fluorescense, [9] and

*To whom correspondence should be addressed. carlos.garcia@utsa.edu, Phone: 01 (210) 458-5774, Fax: 01 (210) 458-5428.

NIH-PA Author Manuscript
NIH-PA Author Manuscript
NIH-PA Author Manuscript

NIH-PA Author Manuscript

NIH-PA Author Manuscript

NIH-PA Author Manuscript

electrochemistry. Among the latter ones, methods based on enzymes immobilized in reactors, [10] microdialysis probes, [11] nanocomposites, [12] or gold surfaces [13] have been reported. Due to the simplicity and miniaturization capabilities of the instrumental setup as well as the potential to provide fast and sensitive detection in both *in vitro* and *in vivo*, amperometry [14–18] isone of the most advantageous ones. In particular, carbon nanotubes (CNT) offer a wide variety of additional advantages in the development of amperometric biosensors [19–22] including high electrode area [23] and good electrical conductivity. Furthermore, recent studies have demonstrated that CNT can enhance the electrochemical reactivity of biomolecules and promote electron transfer reactions. [24–28]

The present paper describes the development of an amperometric biosensor for L-glutamate based on the adsorption of L-glutamate oxidase (GlutOx) on a commercial screen-printed substrate containing the CNT. The experimental conditions to perform the adsorption of the enzyme on the CNT-based substrate were selected based on prior studies performed by our group. [22, 29–31] In addition to providing a robust platform that integrates the working, counter, and reference electrodes, the selected substrate could be easily integrated in a flow-injection analysis (FIA) system, which facilitated sample-handling operations and improved the overall throughput of the analytical method. The following sections provide the characterization of the L-glutamate biosensor and the optimization of experimental conditions in order to maximize its signal. We also demonstrate the use of such sensor for the analysis of glutamate in a real sample (spiked soy sauce).

2. EXPERIMENTAL SECTION

2.1. Regents and Solutions

Aqueous solutions were prepared by using analytical grade regents and ultrapure water (18 MΩ.cm^{-1}, NANOpure Diamond; Barnstead, Dubuque, IA). L-glutamate oxidase (from *Streptomyces* sp., ≥5.0 U.mg^{-1}), H_2O_2, sodium L-glutamate, L-cysteine, acetaminophen, and L-ascorbic acid were purchased from Sigma–Aldrich (Saint Lois, MO). Other chemicals ($NaH_2PO_4 \cdot H_2O$, Na_2HPO_4, HCl, and NaOH) were purchased from Fisher Scientific (Fairlawn, NJ). Sodium phosphate buffer solution (0.10 M, pH=7.4) was prepared daily and used as a background electrolyte for the electrochemical detection as well as a carrier solution in the FIA system. Stock solutions of glutamate (0.10 M) were prepared in phosphate buffer solutions. All experiments were performed at room temperature (22 ± 1 °C).

2.2. Electrochemical Measurements

A CHI-810B workstation (CH Instruments; Austin, TX) was used to characterize the biosensors and to perform the electrochemical detection experiments. In all cases, the commercial screen-printed electrode substrates (DRP-110CNT, DropSens; Asturias, Spain) with 4.0-mm dia. multiwalled CNT-COOH working electrode, carbon ink counter electrode, and an integrated silver pseudo-reference electrode were used. The pseudo-reference electrode developed a potential difference of +20 mV (with respect to a commercial Ag/AgCl/NaCl 3M) when measured in 0.10 M phosphate buffer (pH = 7.4).

2.3. Flow Injection Analysis

The FIA experiments were carried out by using a home-made system that comprised a 12-cylinder peristaltic pump (Gilson Minipuls 3; Middleton, WI), a manual six-port rotary injection valve (Rheodyne 9725; Rohnert Park, CA), and a wall-jet flow cell (DropSens; Asturias, Spain) placed downstream. The injection valve included a 20-μL sample loop (PEEK tubing, 0.020″ ID × 1/16″ OD × 10.1 cm, Upchurch Scientific; Oak Harbor, WA). The wall-jet cell was composed of two transparent methacrylate pieces, an inlet flow

NIH-PA Author Manuscript

NIH-PA Author Manuscript

NIH-PA Author Manuscript

channel that impinged the carrier solution on the detection electrode, and an outlet channel. After the modification of the working electrode with the enzyme solution, the screen-printed electrode substrate was placed in between the cell blocks and connected to the potentiostat using an *ad-hoc* connector. Upon rinsing the system with the carrier solution (to remove the bubbles), the potentiostat was connected, and the baseline current was recorded. Once the baseline was stabilized (< 5 min), solutions containing the selected analyte (L-glutamate or hydrogen peroxide) were injected into the flow stream and the FIA-gram was recorded at a fixed potential. The data points and error bars presented in this manuscript represent the average and standard deviation, respectively, of at least three consecutive injections.

2.4. Preparation of the biosensors

In order to prepare the biosensors, 10.0 μL of a freshly prepared solution of L-glutamate oxidase (≥5.0 $U.mL^{-1}$) was dispensed on the working electrode and incubated at 4 °C overnight. The GlutOx-immobilized electrodes were rinsed with a buffer solution to remove loosely-bound material and stored at 4 °C in pH 7.4 phosphate buffer, solution when not in use.

2.5. Molecular Modeling

The molecular modeling calculations regarding the interaction of the enzyme with the CNT were performed to identify the most likely binding sites. Using AutoDock Vina 4.2, [32] the docking of a 5 nm-long single-wall CNT to GlutOx was computed using the corresponding X-ray crystal structure (PDB ID: 2E1M). [33] A grid box with dimensions of 100 Å in the X, Y, and Z directions was used with the center of the box placed at the center of the protein molecule. Such grid size was selected to include the entire enzyme, therefore allowing the CNT to randomly interact with the whole surface of the protein. The spacing was set at 0.653 Å, defining 1,030,301 points for analysis. The calculation was performed in a MacBook Air (2.13 GHz Intel core duo processor, 4GB RAM memory, and Leopard 10.6.7) and was completed in less than 5 h. Out of the nine potential docking sites, the preferred pose was defined as the one with the minimum potential energy with the maximum number of poses clustered in that site. The graphical analysis of the results was performed with MacPyMol.

3. RESULTS AND DISCUSSION

3.1. Molecular Modeling Studies

In order to gain insight about the potential interaction between CNT and the selected enzyme, preliminary studies were performed using AutoDock Vina. Such docking studies enabled the identification of the most likely manner by which GlutOx was bound to a CNT. As can be observed in Figure 1, the identified docking site involves the interaction of CNT with (mainly) random coil structures in the enzyme. The overall predicted binding energy was −28.0 kcal mol^{-1}, indicating that adsorption process would be sufficient to immobilize GlutOx on the CNT substrate. It is also remarkable that, although these calculations were performed with a single, printine CNT and do not consider effects from the solvent or post-adsorption structural rearrangements of the enzyme, they indicate that the adsorption of enzymes to CNT should not affect the accessibility of the substrate to the active site (Argyr124, Arg305, His312, Gly316, Tyr545, Tyr562, Trp564, and Trp653), [33] therefore enabling the use of this nanocomposite with analytical purposes.

3.2. Characterization of the substrate

In order to gain insight about the morphology of the detection surface, the working electrodes were investigated by scanning electron microscopy (SEM). Figure 2 shows that the electrodes were made of a highly porous matrix with embedded CNT. Based on this

NIH-PA Author Manuscript

NIH-PA Author Manuscript

NIH-PA Author Manuscript

information and recent literature reports obtained with the same type of electrodes [34, 35], it can be concluded that CNT are able to provide a matrix for the immobilization of the enzyme while aiding in the catalysis of H_2O_2. [36] In addition, the presence of the nanopores significantly increased the electrode roughness and therefore the surface area and sensitivity of the biosensor. [23] This increase in surface area in conjunction with the low cost and robustness of these electrodes are very attractive for the development of biosensors for routine applications.

The cyclic voltammetry characterization of these electrodes (data not shown) revealed a wide operational potential window from −0.5 to 1.2 V (vs the included Ag pseudo-reference electrode) with low capacitive current (< 0.6 μA). No redox features (peaks) were observed when cyclic voltammograms were recorded in the background electrolyte solution.

3.3. Effect of detection potential

We have exploited the fact that the H_2O_2 produced in the enzymatic reactions of oxidases can be detected electrochemically under a variety of conditions.[37, 38] Therefore, one of the key parameters in the operation of electrochemical biosensors is the potential applied to the working electrode. Higher potentials typically yield higher signals (currents), but at the expense of selectivity. In order to determine the optimum detection potential, a hydrodynamic voltammogram was obtained by performing sequential injections of 10.0-μM glutamate aliquots into a solution and changing the applied potential in the 0.60–1.20 V range. Figure 3 summarizes the relationship between the peak current and the potential applied to the working electrode for both the L-glutamate and hydrogen peroxide.

It can be seen that the biosensor did not respond to the injection of either L-glutamate or H_2O_2 at potentials lower than 0.7 V. As the detection potential was increased in the 0.7 – 1.1 V window, parallel increases in the peak current for both the L-glutamate and H_2O_2 were observed. These results supported the notion that the glutamate detection was via the oxidation of H_2O_2 that was produced in the enzymatic reaction (1)

$$\text{L-Glutamate} + O_2 + H_2O \xrightarrow{\text{GlutOx}} \text{L-Ketoglutarate} + H_2O_2 + NH_3 \qquad (1)$$

Although the selectivity for electroactive compounds can be limited, an operating potential of 0.95 V was selected and used for the rest of the experiments described in this manuscript. Although electrochemical detection based on reduction of H_2O_2 is also a valid option [39], particularly to decrease the contribution of common interferences, this option typically requires additional modification sof the CNT surface [40, 41] that were considered outside the scope of the present project.

The stability of the signal at 0.95 V was examined by performing consecutive injections of 10.0 μM H_2O_2 (data not shown). Only negligible changes in peak current were observed, which indicated the relevance of screen-printed electrodes as suitable substrates for the development of electrochemical biosensors.

3.4. Effect of flow rate

The effect of flow rate on the response of the biosensor was examined in the 1.0 – 6.0 mL min^{-1} range by performing a series of injections of a solution containing 10.0 μM L-glutamate.

Figure 4 shows that the peak current was higher at lower flow rates. This behavior can be explained by considering that lower flow rates increase the residence time of the analyte in the detection cell, and therefore facilitate the oxidation of a larger number of molecules. It

NIH-PA Author Manuscript

NIH-PA Author Manuscript

NIH-PA Author Manuscript

was also observed, however, that the lower flow rates resulted in the increase of widths of injection peaks (e.g. from 9 ± 1 s at 6.0 mL·min^{-1} to 35 ± 1 s at 1 mL·min^{-1}), which limited the throughput of the technique. In order to preserve a good signal-to-noise ratio along with an acceptable sampling frequency (up to 7 samples min^{-1}), the flow rate of 3.0 mL min^{-1} was selected as optimal and used in all subsequent experiments.

3.5. Effect of pH

The effect of a solution pH on the peak current was investigated in the 6.6 – 8.0 pH range by performing a series of injections of 10.0 μM glutamate solution into the carrier solution. Outside this pH range, a significant enzyme denaturing was observed in accordance with the previous reports. [42]

Figure 5 shows a bell-shaped current-pH curve with a maximum response in the pH range from 7.2 to 7.6. This result matches the optimum pH reported for the free GlutOx enzyme (7.4), [42] which suggests that the enzymatic reaction rather than the electrochemical oxidation of H_2O_2 determines the biosensor's response. In order to maximize the biosensor's response, the pH 7.4 phosphate buffer solution was selected as the optimum carrier solution for all further experiments.

3.6. Analytical figures of merit

Under the optimized experimental conditions, the linear relationship between the L-glutamate concentration and the biosensor's signal (current) extended over the three orders of magnitude (0.01–10 μM). The sensitivity of the method, as defined by the slope of the linear range of the calibration curve, was equal to 0.72 ± 0.05 μA μM^{-1} (R=0.970). The reproducibility of the response was evaluated by recording the peak current obtained upon 50 consecutive injections of 10.0 μM L-glutamate solution into the FIA system. The relative standard deviation of the average peak current was below 6% (data not shown). In order to examine the long-term storage stability, the response of the biosensor was examined by performing 20 consecutive injections of 10.0 μM L-glutamate aliquots every 3 days during a 24-day test period. The biosensor was rinsed with a buffer solution and stored in a pH 7.4 phosphate buffer solution at 4 °C, when not in use. Figure 6 shows that the biosensor retained 92% of its initial signal after 24 days. These results (obtained with a matrix containing CNT) are in good agreement with previous reports stating that although a fraction of the enzymes adsorbed to the CNT surface is denatured, the adsorption of enzymes to CNT is predominantly irreversible [2, 22, 23, 29, 30].

The biosensor's response to some of the most common potential interferences (ascorbic acid, L-cysteine, and acetaminophen) was also investigated. Figure 6 shows that at a concentration level of 100 μM (10 times higher than that of L-glutamate) the interference level of the three species was approximately 3 %. It is also worth noting that, in agreement with previous literature reports, [34] the response of L-cysteine and acetaminophen can be significantly improved under alkaline conditions (data not shown). Unfortunately, under such conditions the catalytic activity of the glutamate oxidase is seriously compromised.

3.7. Determination of L-glutamate in real samples

The biosensor was used to determine the L-glutamate in a real sample of soy sauce. The sample (that contained no MSG) was spiked to a final concentration of 10 μM of L-glutamate and analyzed by the standard addition method using the FIA. It is also worth mentioning that this method was selected due to the presence, in the as-received sample, of other electrochemically-active compounds. Under these conditions, the analysis yielded a calculated concentration of 9.8 ± 0.1 μM (N = 3), which illustrated the merit of the proposed biosensor for the determination of L-glutamate in the matrix of soy sauce.

NIH-PA Author Manuscript

NIH-PA Author Manuscript

NIH-PA Author Manuscript

3.7. Comparison with other electrochemical L-glutamate biosensors

Table 1 shows a comparison of the biosensor presented in this manuscript with other relevant glutamate biosensors published in open literature. Although the new biosensor displays a dynamic range (4 orders of magnitude) that is comparable to other sensors, it features a very low detection limit, which is among the best reported, and a fast response time. Other advantageous features of the proposed platform include the use of a commercially-available electrode substrate combined with the simplicity of enzyme immobilization.

4. CONCLUSIONS

The results described in this paper demonstrate the feasibility of fabricating biosensors by simply adsorbing enzymes on a commercially-available screen-printed substrate modified with carbon nanotubes. Such approach allows for the development of simple and reliable sensors with very low detection limits (nM range). The integration of such biosensors in a flow injection analysis system facilitates the sampling and handling operations such as the injection, detection, and rinsing, which increases the throughput of the technique.

Acknowledgments

Financial support for this project was provided in part by the Welch Foundation Departmental Research Grant (AX-0026) and the National Institutes of Health through the National Institute of General Medical Sciences (1SC3GM081085) and the Research Centers at Minority Institutions (2G12RR013646-11). Dr. R. Khan is thankful to the Department of Science & Technology (DST), Government of India for financial support received under the awarded BOYSCAST Fellowship No. SR/BY/C-09/09. Authors would also like to thank Dr. Murilo Cabral (University of Sao Paulo) for useful discussions and help with AutoDock.

References

1. Jinap S, Hajeb P. Appetite. 2010; 55:1. [PubMed: 20470841]
2. Obrenovitch TP. Ann NY Acad Sci. 1999; 890:273. [PubMed: 10668433]
3. Naylor E, Aillon DV, Gabbert S, Harmon H, Johnson DA, Wilson GS, Petillo PA. J Electroanal Chem. 2011; 656:106.
4. Prescott J, Young A. Appetite. 2002; 39:25. [PubMed: 12160562]
5. Halmos G, Lendvai B, Gáborján A, Baranyi M, Szabó LZ, Csokonai Vitéz L. Neurochem Int. 2002; 40:243. [PubMed: 11741007]
6. Hanko VP, Rohrer JS. Anal Biochem. 2004; 324:29. [PubMed: 14654042]
7. Dawson LA, Stow JM, Palmer AM. J Chromatogr B. 1997; 694:455.
8. Kiba N, Miwa T, Tachibana M, Tani K, Koizumi H. Anal Chem. 2002; 74:1269. [PubMed: 11922293]
9. Doong, R-a; Shih, H-m. Biosen Bioelectron. 2006; 22:185.
10. Hayashi K, Kurita R, Horiuchi T, Niwa O. Biosen Bioelectron. 2003; 18:1249.
11. Morales-Villagrán A, Sandoval-Salazar C, Medina-Ceja L. Neurochem Res. 2008; 33:1592. [PubMed: 18427985]
12. Chakraborty S, Retna Raj C. Electrochem Com. 2007; 9:1323.
13. Muresan L, Nistor M, Gáspár S, Popescu IC, Csöregi E. Bioelectrochem. 2009; 76:81.
14. Chang KS, Hsu WL, Chen HY, Chang CK, Chen CY. Anal Chim Acta. 2003; 481:199.
15. Khampha W, Meevootisom V, Wiyakrutta S. Anal Chim Acta. 2004; 520:133.
16. Oliveira MIP, Pimentel MC, Montenegro MCBSM, Araújo AN, Pimentel MF, Silva VLd. Anal Chim Acta. 2001; 448:207.
17. Zhang M, Mullens C, Gorski W. Electrochim Acta. 2006; 51:4528.
18. Zhang M, Mullens C, Gorski W. Electroanalysis. 2005; 17:2114.
19. Lin Y, Lu F, Wang J. Electroanalysis. 2004; 16:145.

NIH-PA Author Manuscript

NIH-PA Author Manuscript

NIH-PA Author Manuscript

20. Wang Z, Liu J, Liang Q, Wang Y, Luo G. Analyst. 2002; 127:653. [PubMed: 12081044]
21. Zhao YD, Zhang WD, Chen H, Luo QM. Talanta. 2002; 58:529. [PubMed: 18968780]
22. Mora MF, Giacomelli CE, Garcia CD. Anal Chem. 2009; 81:1016. [PubMed: 19132842]
23. Nejadnik MR, Francis L, Garcia CD. Electroanalysis. 2011; 23:1462.
24. Tang L, Zhu Y, Xu L, Yang X, Li C. Talanta. 2007; 73:438. [PubMed: 19073053]
25. Tang L, Zhu Y, Yang X, Li C. Anal Chim Acta. 2007; 597:145. [PubMed: 17658324]
26. Zhang M, Gorski W. Anal Chem. 2005; 77:3960. [PubMed: 15987097]
27. Zhang M, Smith A, Gorski W. Anal Chem. 2004; 76:5045. [PubMed: 15373440]
28. Wooten M, Gorski W. Anal Chem. 2010; 82:1299. [PubMed: 20088562]
29. Felhofer JL, Caranto J, Garcia CD. Langmuir. 2010; 26:17178. [PubMed: 20945910]
30. Valenti LE, Fiorito PA, Garcia CD, Giacomelli CE. J Colloid Interface Sci. 2007; 307:349. [PubMed: 17174970]
31. Wehmeyer J, Bizios R, Garcia CD. Mat Sci Eng C. 2010; 30:277.
32. Trott O, Olson AJ. J Comp Chem. 2010; 31:455. [PubMed: 19499576]
33. Arima J, Sasaki C, Sakaguchi C, Mizuno H, Tamura T, Kashima A, Kusakabe H, Sugio S, Inagaki K. FEBS J. 2009; 276:3894. [PubMed: 19531050]
34. Fanjul-Bolado P, Hernández-Santos D, Lamas-Ardisana PJ, Martín-Pernía A, Costa-García A. Electrochim Acta. 2008; 53:3635.
35. Kadara RO, Jenkinson N, Banks CE. Sens Actuators B. 2009; 138:556.
36. Fanjul-Bolado P, Queipo P, Lamas-Ardisana PJ, Costa-García A. Talanta. 2007; 74:427. [PubMed: 18371659]
37. Blanes L, Mora Maria F, do Lago Claudimir L, Ayon A, Garcia Carlos D. Electroanalysis. 2007; 19:2451.
38. Nejadnik MR, Garcia CD. Colloids Surf B. 2011; 82:253.
39. Karyakin AA, Gitelmacher OV, Karyakina EE. Anal Chem. 1995; 67:2419.
40. Salimi A, Compton RG, Hallaj R. Anal Biochem. 2004; 333:49. [PubMed: 15351279]
41. Santhosh P, Manesh KM, Lee KP, Gopalan AI. Electroanalysis. 2006; 18:894.
42. Sukhacheva M, Netrusov A. Microbiology. 2000; 69:17.
43. Ammam M, Fransaer J. Biosen Bioelectron. 2010; 25:1597.
44. Rahman MM, Umar A, Sawada K. J Phys Chem B. 2009; 113:1511. [PubMed: 19143491]
45. Meng L, Wu P, Chen G, Cai C, Sun Y, Yuan Z. Biosen Bioelectron. 2009; 24:1751.
46. Noda T, Ukai T, Yao T. Anal Sci. 2010; 26:675. [PubMed: 20543499]

NIH-PA Author Manuscript

NIH-PA Author Manuscript

NIH-PA Author Manuscript

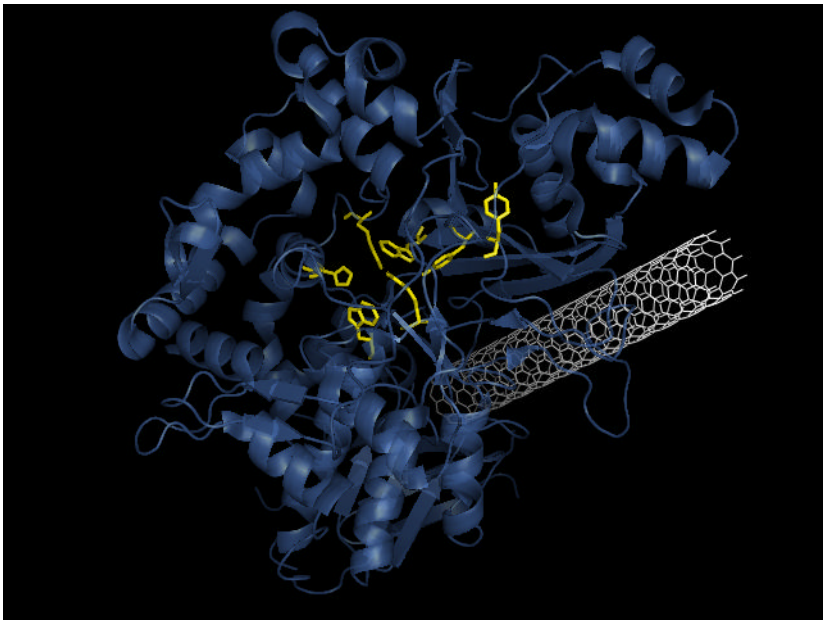

Figure 1.
Binding pose of GlutOx on CNT, as calculated using molecular docking (AutoDock Vina). The figure also highlights (yellow) the amino acids defining the active site of the protein.

NIH-PA Author Manuscript

NIH-PA Author Manuscript

NIH-PA Author Manuscript

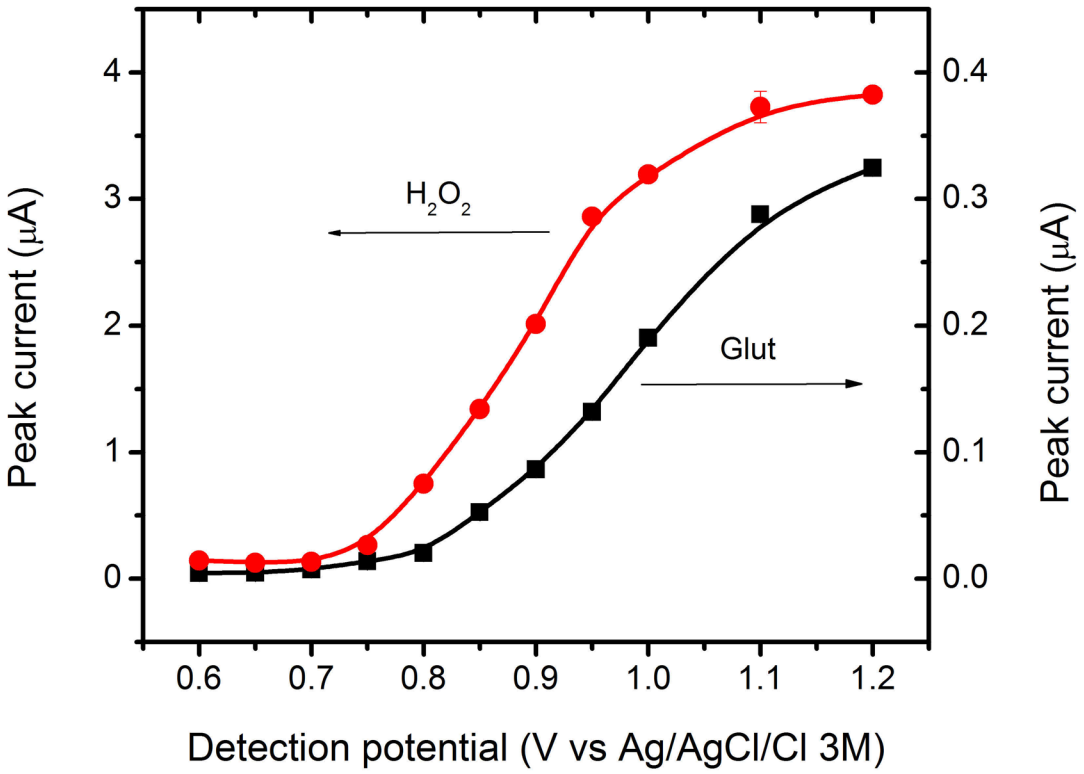

Figure 2.
SEM micrograph of the surface of the screen printed electrodes containing multi-wall CNT.

NIH-PA Author Manuscript

NIH-PA Author Manuscript

NIH-PA Author Manuscript

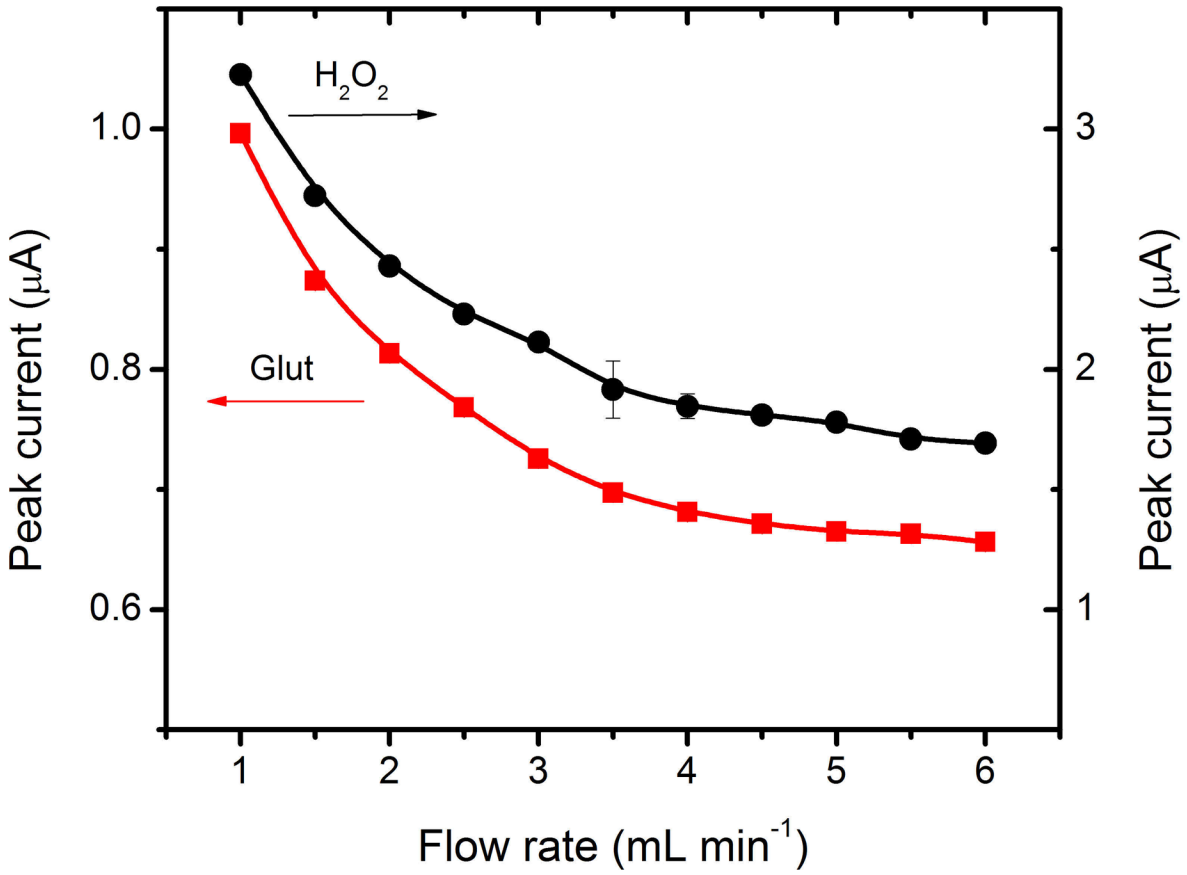

Figure 3.

Hydrodynamic voltammograms of (a) 10 μM L-Glutamate, and (b) 10 μM H_2O_2 recorded at the biosensor. Carrier solution, pH 7.4 phosphate buffer (0.10 M). Flow rate, 3.0 ml min^{-1}.

NIH-PA Author Manuscript

NIH-PA Author Manuscript

NIH-PA Author Manuscript

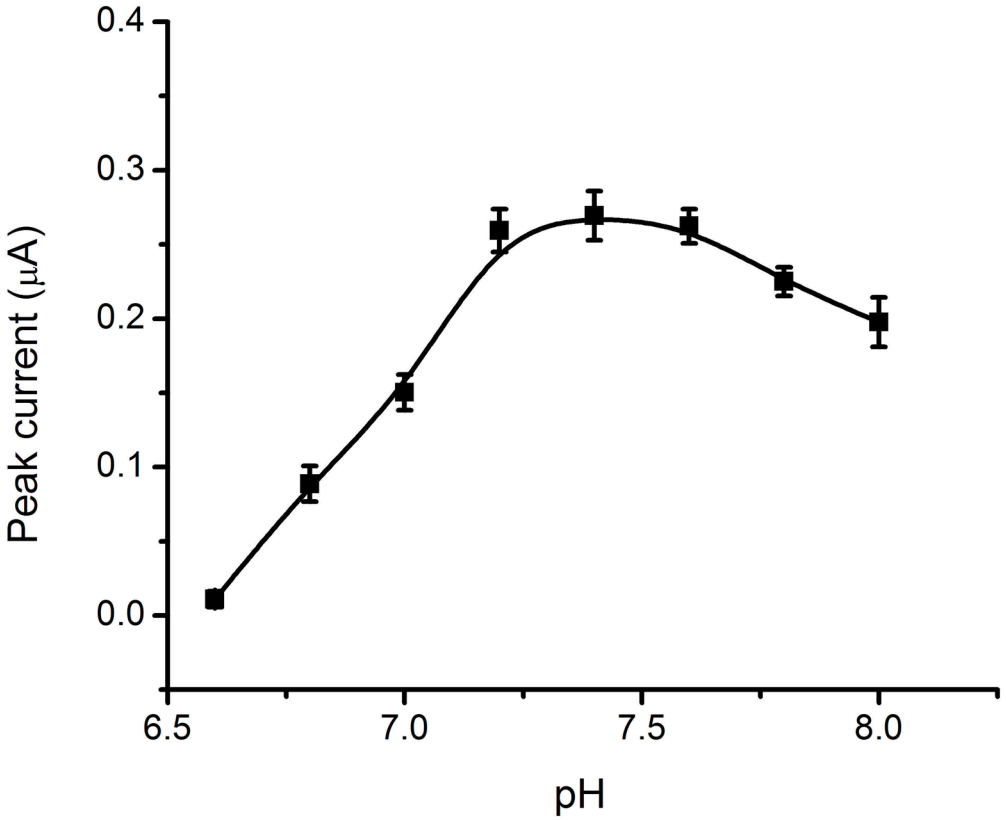

Figure 4.
Effect of flow rate on the current response of the biosensor to (a) 10.0 μM L-glutamate, and (b) 10 μM H_2O_2. Carrier solution, pH 7.4 phosphate buffer (0.10 M). Potential, 0.95 V.

NIH-PA Author Manuscript

NIH-PA Author Manuscript

NIH-PA Author Manuscript

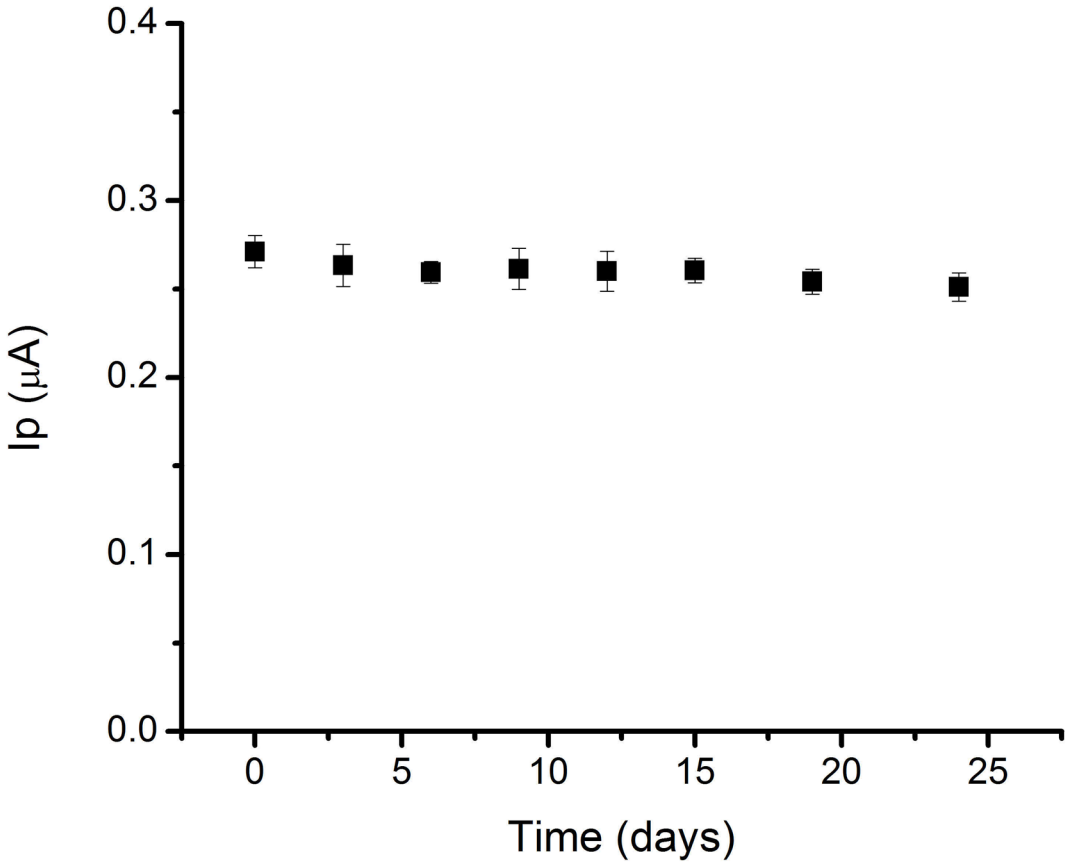

Figure 5.

Effect of pH on the amperometric response of the biosensor to 10.0 μM L-glutamate. Carrier solution, pH 7.4 phosphate buffer (0.10 M). Flow rate, 3.0 ml min^{-1}. Potential, 0.95 V.

NIH-PA Author Manuscript

NIH-PA Author Manuscript

NIH-PA Author Manuscript

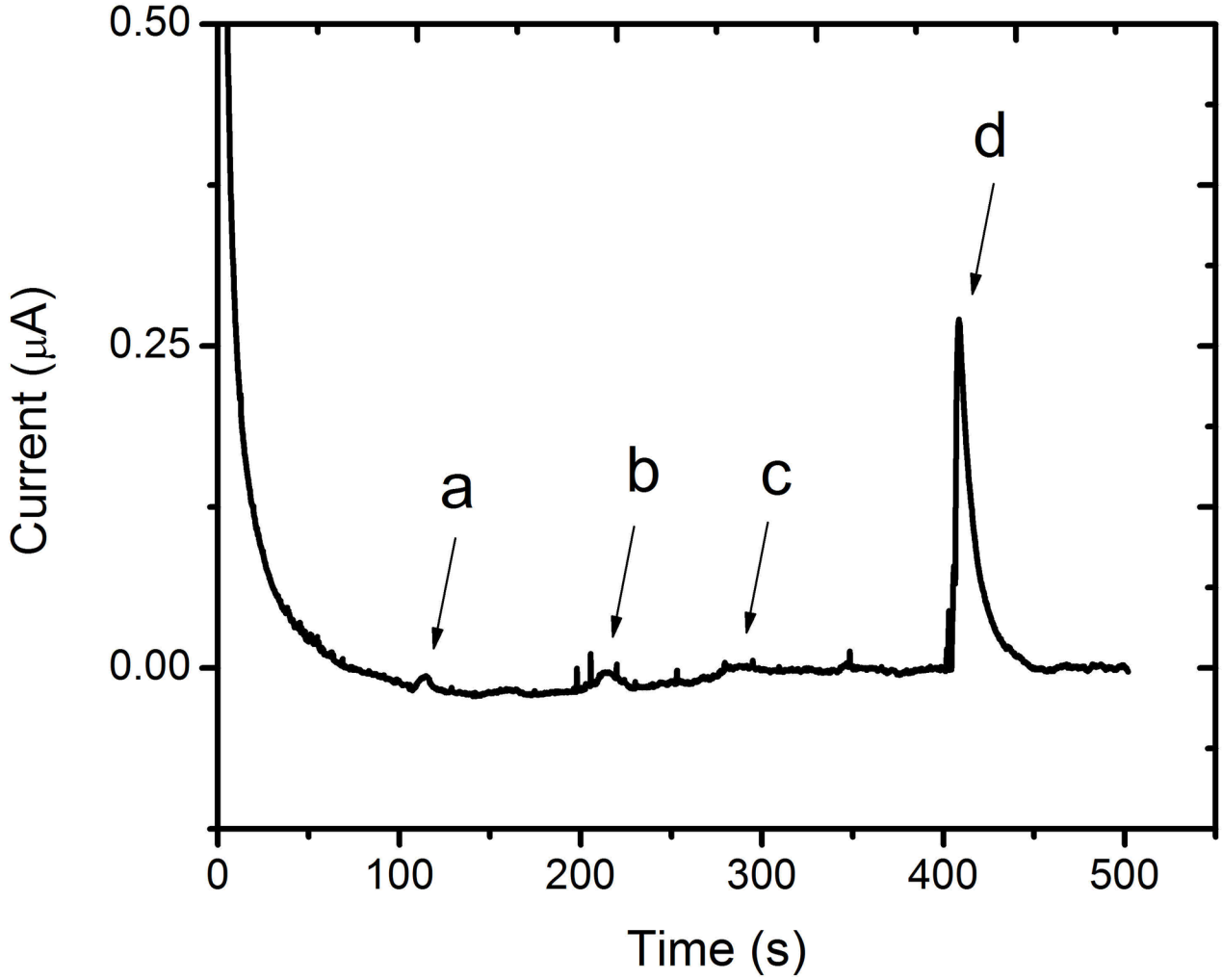

Figure 6.
Shelf-stability of the biosensor measured by sequential injections of 10.0 μM L-glutamate solution into a carrier solution. Carrier solution, pH 7.4 phosphate buffer (0.10 M). Flow rate, 3.0 ml min^{-1}. Potential, 0.95 V.

NIH-PA Author Manuscript

NIH-PA Author Manuscript

NIH-PA Author Manuscript

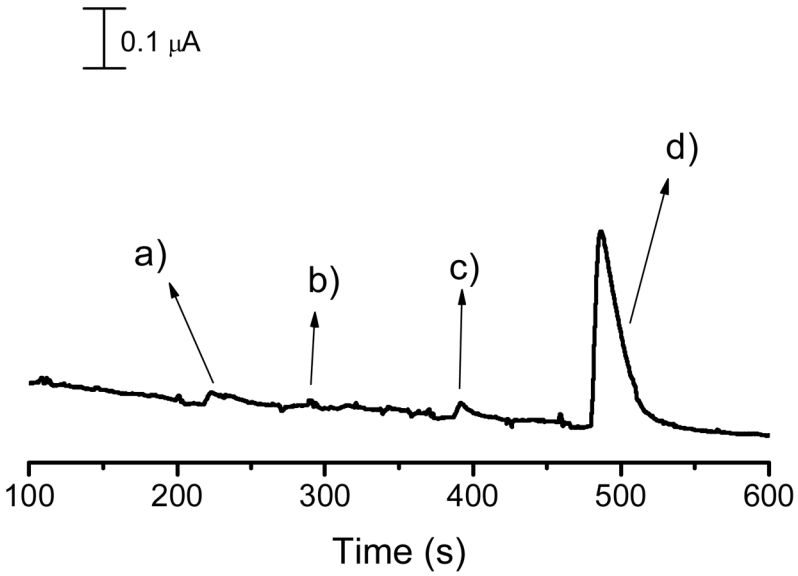

Figure 7.

Amperometric trace recorded at the biosensor (a) 100 μM ascorbic acid, (b) 100 μM L-cysteine, (c) 100 μM acetaminophen, and (d) 10 μM L-glutamate. Carrier solution, pH 7.4 phosphate buffer (0.10 M). Flow rate, 3.0 ml min^{-1}. Potential, 0.95 V.

NIH-PA Author Manuscript

NIH-PA Author Manuscript

NIH-PA Author Manuscript

Table 1

Comparison of selected electrochemical biosensors for L-glutamate

Electrode	E_{DET} (V)	Linear range (μM)	Response time (s)	Ref.
SPE	0.95 [a]	0.01 – 10	5	This work
CNT/Chitosan	0.40 [b]	0.5 – 200	2	[17]
CNT/Chitosan	0.40 [b]	0.5 – 500	2	[18]
(Pt-PAMAM)nCNTs	0.20 [b]	0.2 – 250	3	[24]
Pt-DENs/CNTs/Ppy	0.20 [b]	0.1 – 60	3	[25]
PPy/MWCNT	1.10 [b]	0.3 – 140	7	[43]
Th-MWCNTs	0.145 [b]	0.1 – 500	3	[44]
Th-SWNTs	0.19 [b]	0.5 – 400	5	[45]
CSCNTsGC	0.0 [b]	0.003 – 10	-	[46]

[a] vs integrated pseudo-reference electrode,

[b] vs. Ag/AgCl/3M NaCl reference electrode,

SPE: screen printed electrode, PAMAM: Poly(amido amine), DENs: dendrimers, Ppy: Polypyrrole; MWCNT: multi-wall carbon nanotubes, SWCNT: single-wall carbon nanotubes, CSCNT: cup-stacked, GC: glassy carbon.